# Simulated global HYCOM (GLBa0.24) results from various ocean color forcings: Preliminary results from sensitivity analyses

Hae-Cheol Kim[1,*], Avichal Mehra[2], Sudhir Nadiga[1], Zulema Garraffo[1], Seunghyun Son[3]
[1]IMSG at NWS/NCEP/EMC, [2]NWS/NCEP/EMC, [3]CIRA at NESDIS
Email: Hae-Cheol.Kim@noaa.gov; Phone: 301-683-3761

Chlorophyll *a* (Chl-*a*) is one of the most commonly used biomass indicators in marine phytoplankton ecology. Phytoplankton are primary producers of organic materials, and in the upper ocean, have their own internal physical and biogeochemical (BGC) dynamics. Along with photosynthesis, another major aspect of phytoplankton in the upper ocean is their role in attenuating radiant fluxes through optical processes such as absorption and scattering. Chlorophyll *a* and its attenuation characteristics can be estimated through remote sensing techniques. Despite the reality that observations are limited to 2-dimensional surface fields, remotely-sensed ocean color data (Chl-*a* concentration and the diffuse attenuation coefficients at 490 nm ($K_{d490}$) and for photosynthetically available radiation ($K_{dPAR}$)) have been by far the most easily accessible and most frequently used products for providing an up-to-date state of marine primary producers (phytoplankton) and their photosynthetic activity (primary production). This bottom-up control is critical to understanding the dependent oceanic food webs in a region and the biogeochemical cycles relevant to global processes. In addition, data assimilation of ocean color products (e.g., SeaWiFS, MODIS, VIIRS) will provide a unique and timely opportunity to establish a path toward ecological forecasting through biogeochemical analyses and forecasts.

As a component of initial efforts to test operational feasibility and capability, we investigated the effects of various ocean color products on ocean model behaviors and its upper ocean thermal structure. We used a 1/4$^o$ Hybrid Coordinate Ocean Model (HYCOM; GLBa0.24 hereafter) with cylindrical (78.64°S – 66°S); recti-linear coordinate (66°S – 47°N); and. Arctic bipolar patch (>47°N). It has vertical coordinates employing 32 layers with following isopycnals in the deep sea, z-levels in the surface and a terrain-following σ-coordinate near coastal areas [1]. K-Profile Parameterization (KPP) [2] is used as a vertical mixing scheme. GLBa0.24 was forced by hourly atmospheric fluxes from NOAA's Climate Forecast System Reanalysis (CFSR) [3]. Four numerical experiments were set up by combining three different ocean color products and two shortwave radiant flux algorithms (Table 1).

Table 1. Various ocean color products used by RTOFS-Global for short wave radiant fluxes.

| Experiments | Ocean color product | Sensor | Period | Algorithms |
|---|---|---|---|---|
| KparCLM | Long-term climatological $K_{dPAR}$ [4] | SeaWiFS | 1997-2010 | [5] |
| ChlaCLM | Long-term climatological Chl-*a* [6] | SeaWiFS | 1997-2010 | [7] |
| ChlaIND | Interannual mean Chl-*a* [6] | SeaWiFS | Each year (2001 – 2010) | [7] with no diurnal variation |
| ChlaID | Interannual mean Chl-*a* [6] | SeaWiFS | Each year (2001 – 2010) | [7] with diurnal variation |

KparCLM is based on a 13-year long-term climatological $K_{dPAR}$ derived from SeaWiFS [4]. The algorithm to compute shortwave radiant fluxes is based on $K_{dPAR}$ [5]. ChlaCLM is based on a 13-year long-term Chl-*a* derived from SeaWiFS [6] and the shortwave radiation algorithm used in this experiment directly uses Chl-*a* to compute inherent (*a*: absorption coefficients) and apparent optical properties ($K_d$: downwelling attenuation coefficient; $\theta$: solar zenith angle) [7]. ChlaIND and ChlaID use the same ocean color forcing, interannual mean of SeaWiFS Chl-*a* but the former experiment does not consider the diurnal effects of solar zenith angle, whereas the latter included diurnal changes of the Sun's incident angle (0$^o$ to 60$^o$ as described in [7]). In summary, the comparison between KparCLM and ChlaCLM gives algorithmic differences; the comparison between ChlaCLM and ChlaIND gives effects of mesoscale variabilities; and the comparison between ChlaIND and ChlaID yields diurnal variabilities and short-term

scale effects. All experiments were initialized at January 1, 2001 and ran for 10 years. Surface temperature values are not constrained to data (no surface relaxation to climatology).

Figures 1 and 2, respectively, represent a snapshot of differences in sea surface height (SSH) and sea surface temperature (SST) between the experiments one year after the initialization. Differences are noticeable in the areas of surface boundary currents, such as Kuroshio Current, Gulf Stream, Benguela Current, and Antarctic Circumpolar Current. The Equatorial Pacific also revealed basin-wide noticeable changes in both SSH and SST. It is noteworthy that the algorithmic difference (Figs.1a and 2a) created larger scale changes compared to other comparisons (e.g., changes in SSH in the Southern Ocean area; basin-wide changes in Pacific Ocean SST). Although it is apparent that the sensitivity of different ocean color products and optical algorithms made noticeable changes, more robust statistical analyses are required to confirm these synoptic findings in the comparisons.

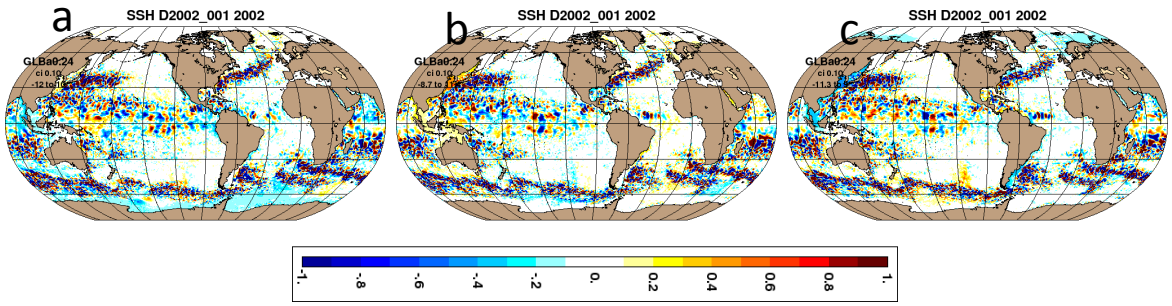


Fig. 1. Differences in SSH between KparCLM and ChlaCLM (a); ChlaCLM and Expt03.2 (b); and ChlaIND and ChlaID (c).

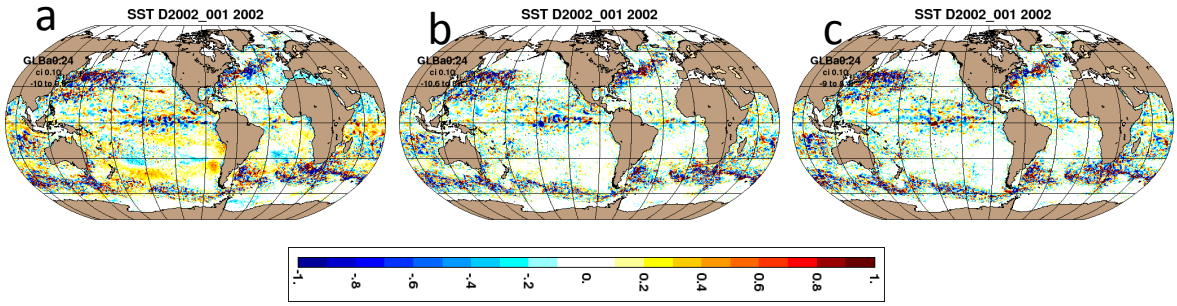


Fig. 2. Differences in SST between KparCLM and ChlaCLM (a); ChlaCLM and Expt03.2 (b); and ChlaIND and ChlaID (c).

[1] Bleck, R., 2002: An oceanic general circulation model framed in hybrid isopycnic-Cartesian coordinates, Ocean Model., 37, 55-88.
[2] Large, W.C., J.C. McWilliams and S.C. Doney, 1994: Oceanic vertical ixing: a review and a model wit a nonlocal boundary layer parameterization. Rev. Geophys. 32, 363-403.
[3] Saha, S., *et al.* (2010) The NCEP climate forecast system reanalysis. Bull. Amer. Meteor. Soc., 91, 1015–1057.
[4] Son, S. and M. Wang (2015) Diffuse attenuation coefficient of the photosynthetically available radiation Kd(PAR) for global open ocean and coastal waters, Remote Sens. of Environ., 159, 250-258.
[5] Kara, A.B., H.E. Hurlburt, P.A. Rochford, and J.J. O'Brien (2004). The impact of water turbidity of the interannual sea surface temperature simulations in a layered global ocean model. J. Phys. Oceanogr., 34, 345–359.
[6] O'Reilly, J.E., S. Maritorena, B.G. Mitchell, D.A. Siegel, K L. Carder, S. A. Garver, M. Kahru, and C. McClain (1998), Ocean color chlorophyll algorithms for SeaWiFS, J. Geophys. Res., 103, 24,937-24,954.
[7] Lee, J., K. Du, R. Arnone, S. Liew, and B. Penta (2005), Penetration of solar radiation in the upper ocean: A numerical model for oceanic and coastal waters, J. Geophys. Res., 110, 1-12.